

# Neutron irradiation and light transmission assessment of plastic scintillators of the TileCal section of the ATLAS detector.

**J E Mdhuli<sup>1</sup>, R Erasmus<sup>1</sup>, Y U Davydov<sup>2</sup>, H Jivan<sup>1</sup>, S Liao<sup>1</sup>, C Pelwan<sup>1</sup>, E Sideras-Haddad<sup>1</sup>, B Mellado<sup>1</sup>, G Peters<sup>1</sup> and C Sandrock<sup>1</sup>**

<sup>1</sup>University of the Witwatersrand, 1 Jan Smuts Avenue, Braamfontein 2000, Johannesburg.

<sup>2</sup>Joint Institute for Nuclear Research (JINR), Dubna, Russia.

E-mail: joyemmie@gmail.com

**Abstract.** Following the comparative study of proton induced radiation damage on various plastic scintillator samples from the ATLAS detector [1][3-5], a study on neutron irradiation and damage assessment on the same type of samples is currently being conducted. The samples were irradiated with different neutron fluxes produced in favourable nuclear reactions using the IBR-2 pulsed reactor at the Joint Institute for Nuclear Research (JINR) in Dubna. The MCNP 5 code was utilized in simulating the neutron transport for determining the dose rate. Light transmission tests were performed in order to assess the radiation damage on the scintillators. The first results of the effect of neutron irradiation on the transmission properties of a number of plastic scintillator materials is presented.

## 1. Introduction

The ATLAS detector is used to measure what happens in proton-proton collisions at the Large Hadron Collider (LHC) to find evidence of new physics. The tile calorimeter is part of the ATLAS detector, it is the hadronic calorimeter responsible for detecting hadrons, taus, and jets of quarks and gluons. The tile calorimeter consists of a central barrel and 2 extended barrels. Each barrel contains 64 modules that consists of a matrix of steel plates and plastic scintillators. The steel plates act as an absorber medium that converts the incoming jets into a shower of particles. The plastic scintillator tiles then absorb the energy of the particles and fluoresce to emit light. The light from the scintillators is passed through wavelength shifting optical fibres and is detected by photomultiplier tubes. The signal is further processed using readout electronics in order to digitize the data for further analysis [1][2].

Between the central barrel and extended barrels there is what is referred to as the Gap region. This region contains additional plastic scintillators that are radially distributed. During the first run of data taking, the scintillators in the gap region were exposed to a radiation environment of up to 10 kGy/year. It is predicted that during the high luminosity (HL)-LHC run time, the scintillators in the Gap region will sustain a significantly large amount of radiation damage and will require replacement during the phase 2 upgrade in 2018. This prediction has led to the comparative study of proton induced radiation damage on plastic scintillators conducted by H Jivan [1][3], C Pelwan [4] and S Liao [5].

With 2018 rapidly approaching, the comparative study of proton irradiated plastic scintillators

has been extended to study the effect of neutron induced radiation damage on plastic scintillators. In this paper, we report some of the results obtained from radiation damage induced by neutron irradiation.

Neutron interaction with matter makes the study more interesting since unlike with proton irradiation where the interaction with the plastics is through direct ionization, with neutron irradiation the interaction will be through indirect ionization. Neutron bombardment on materials creates a collision cascade within the material that results to point defects and dislocations. The collisions cause a massive transfer of kinetic energy to the lattice atom that has been displaced from its lattice site, becoming what is known as the primary knock-on atom (PKA). The knock-on atoms then lose energy with each collision and that energy therefore ionizes the material [6].

## 2. Scintillation Mechanism

The plastic scintillator samples that were studied are organic scintillators, these scintillators have a basic scintillation mechanism that involves Föoster energy transfer and self-absorption. They consist of one or two dopants. The scintillation mechanism of organic scintillators is determined by the characteristics of the benzene ring. An organic scintillator scintillates regardless of its crystal form, whether it be a liquid, a gas or imbedded in a polymer. The chemical bonds found within a benzene ring are:  $\sigma$ -bonds that are in the plane with bond angle  $120^\circ$  and are from  $sp^3$  hybridization. The other chemical bonds found are  $\pi$ -orbitals which are out of plane and overlap. The  $\pi$ -electrons are completely delocalized.

Looking at the scintillation mechanism after the scintillator has absorbed the photon or excitation by ionization, the molecule will undergo vibrational relaxation to the  $S_{10}$  state. The  $S_{10}$  excited state radiatively decays to the vibrational sub-levels of the ground state. The lifetime of the  $S_{10}$  state is in the nanoseconds time range. The short lifetime allows for the fluorescence emission spectrum to be roughly a mirror image of the absorption spectrum, in other words, they have the same spacing. The emitted photons have less energy than the  $S_{00}$ - $S_{10}$  phase transition and that's where the important Stokes shift is observed. There is no  $S_2$ - $S_0$  emission, thus there is an internal non-radiatively de-excitation occurring within the scintillator taking place in the picoseconds time range and, the excited triplet state cannot decay to the ground state as a result angular momentum selection rules, it therefore results in a delayed fluorescence and phosphorescence [7]. This is clearly illustrated in figure 1.

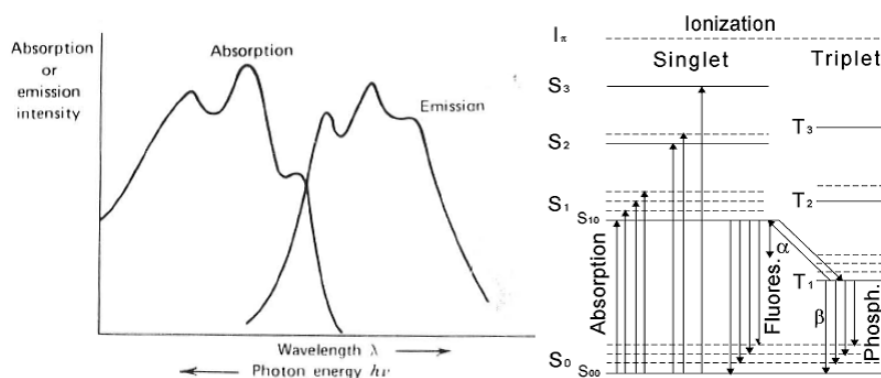


**Figure 1.** A fluorescence absorption and emission spectra (left) and scintillation mechanism for an organic scintillator (right) [7].

### 3. Experimental Details

Four plastic scintillator grades were under study, three of which were obtained from ELJEN technologies and one from Dubna. The three plastic scintillators obtained from ELJEN technologies are composed of a polyvinyl toluene base and 3% added organic fluors [1], the fourth plastic scintillator grade is the Kharkov (UPS923A) type manufactured by the Institute for Scintillation Materials (ISMA). The plastic scintillator grades under study are the EJ200, EJ208, EJ260 and the UPS923A.

Several samples of each plastic scintillator grade were cut and polished at the Dzhelapov Laboratory of Nuclear Problems (DLNP) at JINR. Sixteen samples were cut to dimensions 20 mm by 20 mm, with 6 mm thickness. Special sample holders were made to accommodate our samples due to their size. Channel 3 of the IBR-2 pulsed reactor at the Frank Laboratory of Neutron Physics (FLNP) in JINR was used to irradiate the samples [8]. The samples were subjected to irradiation with a beam of fast neutrons with energies  $\geq 1$  MeV for 337 hours, the length of the April Run 2016. The reactor was operating at an average power of 1875 kW. The samples were placed at three different positions from the reactor core to expose the samples to different neutron fluxes to achieve various doses. The neutron flux density ranged between  $1 \times 10^6 \sim 7.7 \times 10^6$   $n/cm^2/s$ .

Taking into account the reactor spectrum, the Monte Carlo N-Particle (MCNP) 5 [9] code was used to simulate neutron transport through plastic scintillators and to determine the dose rate. The Monte Carlo method is used to simulate statistical processes theoretically, in particular complex problems that cannot be solved/modelled using computer codes that use deterministic methods. Table 1 shows the neutron flux density, neutron fluences and doses at the various positions.

**Table 1.** Neutron flux density, neutron fluences and doses at the various positions.

Sample number	Flux density ( $n/cm^2/s$ )	Fluence ( $n/cm^2$ )	Dose ( $Gy$ )
1, 5, 12, 19	$1.0 \times 10^6$	$1.2 \times 10^{12}$	66
2, 6, 13, 20	$3.6 \times 10^6$	$3.6 \times 10^{12}$	199
3, 7, 14, 21	$7.7 \times 10^6$	$9.4 \times 10^{12}$	510

Light spectroscopy was conducted using the Varian Carry 500 spectrophotometer to characterize the optical properties of the irradiated samples due to the damage of the neutron irradiation. The light transmission of the samples was measured relative to the transmission in air over a laser wavelength range between 200-800nm. Transmission spectra were collected a few weeks after irradiation, control samples were left un-irradiated in order to gauge the transmission loss.

### 4. Light Transmission Results and Analysis

The light transmission spectroscopy results for each scintillator grade relative to the light transmission in air are shown below on the spectra on the left in Figures 2-5. In Figure 2, it is observed that at a wavelength of 400 nm the absorptive edge falls away completely for the EJ200 grade. Figure 3 shows the light transmission spectrum of the EJ208 grade. It is observed from the spectrum that the absorptive edge falls away at 385 nm. At the highest exposed neutron flux density, there is an increase in transmission. At neutron flux densities lower than  $3.6 \times 10^6$   $n/cm^2/s$ , there is a decrease in light transmission. We observe a relative increase in transmission above  $\sim 700$  nm for samples EJ200 and EJ208. The transmission spectrum for the EJ260 is shown in Figure 4, it is observed that transmission starts to occur at wavelength 355 nm for a short wavelength range as seen from the mini peak on the spectrum. The absorptive edge

falls away completely at 460 nm. The overall transmission of the grade decreases with radiation damage. Figure 5 shows the transmission spectrum of the UPS932A grade, the absorptive edge for this grade falls off completely at 400 nm. It is observed that the overall transmission of the grade increases with increasing dose.

The transmission loss is observed at wavelength 450 nm as this corresponds to the peak absorption wavelength of the wavelength shifting optical fibres coupled with these scintillators within the Tile Calorimeter. We consider the transmission loss of the highest neutron flux density  $7.7 \times 10^6 \text{ n/cm}^2/\text{s}$ . We observe a 3.4% transmission loss for the EJ200, 3% transmission increase for the EJ208 and no transmission loss for the EJ260 as the sample absorbs light in the wavelength range from 400 nm to 460 nm. The UPS932A grade shows a 2.9% transmission increase. The transmission loss is clearly shown in Figures 2-5 on the spectra on the right.

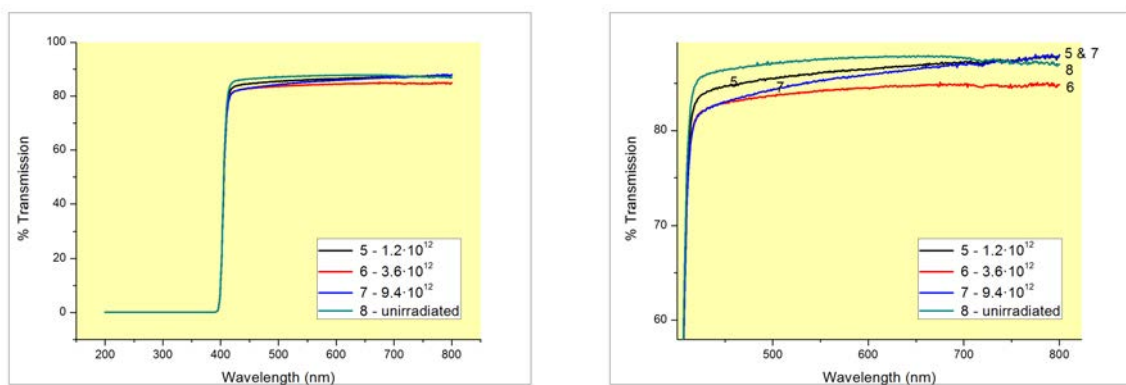


**Figure 2.** Left: Transmission spectrum for un-irradiated and irradiated samples for the EJ200 grade. Right: Enlarged spectrum at wavelength 400 800 nm.

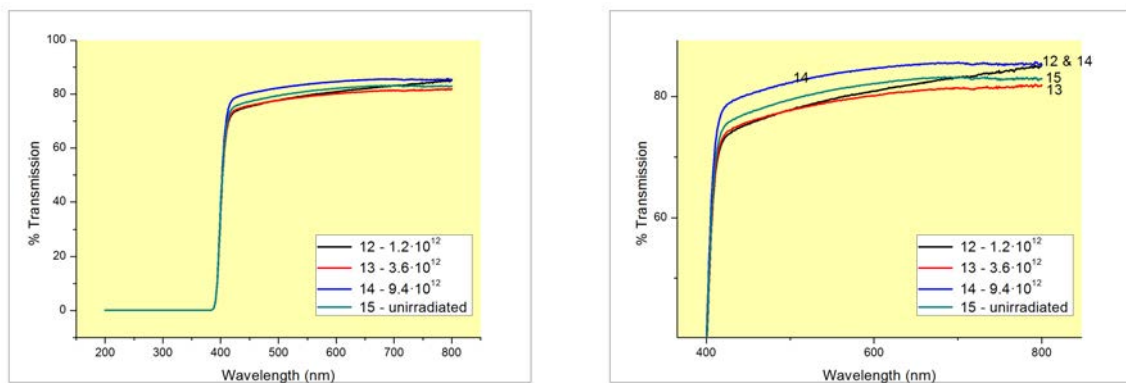


**Figure 3.** Left: Transmission spectrum for un-irradiated and irradiated samples for the EJ208 grade. Right: Enlarged spectrum at wavelength 400 800 nm.

### 5. Conclusion

From the results obtained in this study, neutron irradiation has indeed have an observable effect on the light transmittance of plastic scintillators. We considered the transmission loss at wavelength of approximately 450 nm which corresponds to the peak absorption wavelength of the

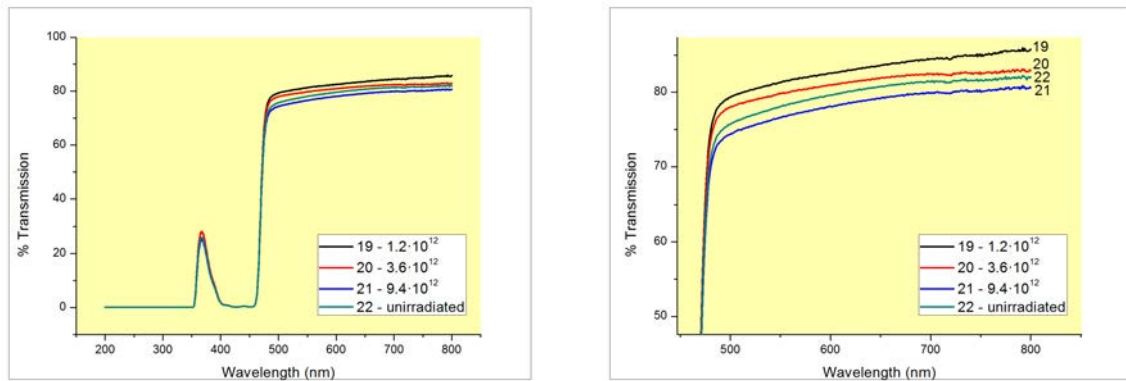


**Figure 4.** Left: Transmission spectrum for un-irradiated and irradiated samples for the EJ260 grade. Right: Enlarged spectrum at wavelength 460 800 nm.

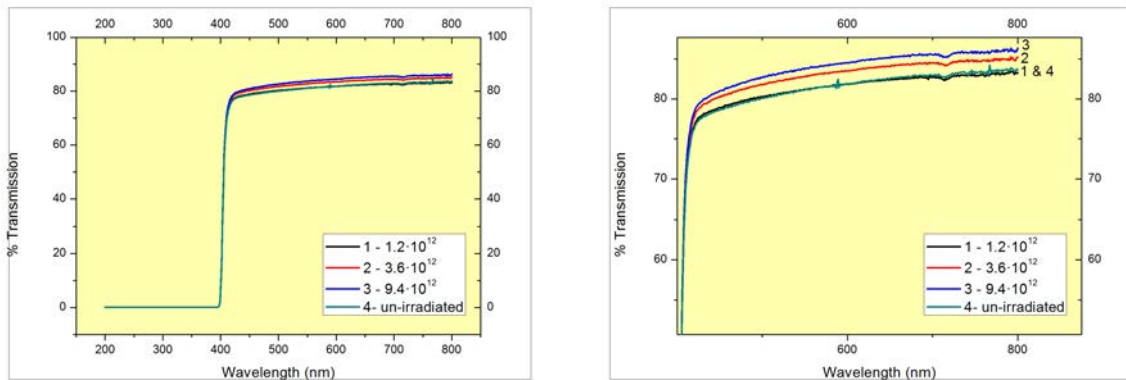


**Figure 5.** Left: Transmission spectrum for un-irradiated and irradiated samples for the UPS932A grade. Right: Enlarged spectrum at wavelength 400 800 nm.

wavelength shifting optical fibres coupled with these scintillators within the Tile Calorimeter. The EJ200 showed the highest transmission loss with a 3.8% loss whilst for the EJ260 no transmission occurs in the wavelength range of 400 460 nm. Unlike the EJ200 and EJ260, the EJ206 and the UPS932A have an increase in transmittance by 3% and 2.9% respectively. The overall transmission for the EJ200 and EJ260 decreases with exposure to radiation but there is no clear relationship between the neutron flux density and the light transmittance from the neutron flux densities under study. For the EJ208 and UPS932A, the highest neutron flux density shows an increase in transmittance. The highest neutron flux density shows an increase in light transmission whilst neutron flux density below  $3.6 \times 10^6 \text{ n/cm}^2/\text{s}$  show that there is a transmission loss for the EJ208. The Kharkov grade shows transmission loss for the lowest neutron flux density, below  $1.0 \times 10^6 \text{ n/cm}^2/\text{s}$  and an increase in transmission for neutron flux density above  $3.6 \times 10^6 \text{ n/cm}^2/\text{s}$ . No additional features were observed on the spectra due to radiation damage for all the grades compared to those observed in the proton irradiated samples [1].

All the results in this study are preliminary, they will be used as a guide in future studies. No conclusions can be made in this study on which plastic scintillator grade performed better under neutron radiation.

## 6. Upcoming Work

Light yield tests will be done next. Raman spectroscopy will also be performed to observe if any structural damage occurred from the radiation damage. More samples will be irradiated at higher exposure doses to study on how the plastic scintillators behave higher doses of radiation damage. A study on the thickness dependence of the plastic scintillators will also be conducted. This will focus on studying the relationship between the thickness and the transmittance of the sample after undergoing radiation damage.

The project aims to extend these studies to include radiation assessment damage of any component that processes the scintillating light and deteriorates the quantum efficiency of the Tilecal detector, namely, photomultiplier tubes, wavelength shifting optical fibres and readout electronics will also be exposed to neutron irradiation and the damage will be assessed in the same manner. The linear accelerator and the SAFARI-1 reactor will also be used to irradiated the samples under study.

### Acknowledgements

We would like to acknowledge the technical staff at the Dzhelapov Laboratory of Nuclear Problems (DLNP) and Frank Laboratory of Neutron Physics (FLNP) at the Joint Institute for Nuclear Research (JINR) for all their assistance and allowing us to use their laboratories.

## References

- [1] Jivan H, Erasmus R, Mellado B, Peters G, Sekonya K, Sideras-Haddad E. 2015. "Radiation hardness of plastic scintillators for the Tile Calorimeter of the ATLAS detector." *Journal of Physics conference series* **645**
- [2] Succurro A 2012. "The ATLAS Tile Hadronic Calorimeter performance in the LHC collision era." *Physcis Procedia* **37** 229 - 237.
- [3] Jivan H, Mellado B, Sideras-Haddad E, Erasmus R, Liao S, Madhuku M, Peters G, Solvyanov O. 2015. "Radiation hardness of plastic scintillators for the Tile Calorimeter of the ATLAS detector." *Journal of Physics conference series* **623**.
- [4] Pelwan C, Jivan H, Joubert D, Keartland J, Liao S, Peters G, Sideras-Haddad E. 2015. "Characterization of plastic scintillators using magnetic resonance techniques for the upgrade of the Tile Calorimeter in the ATLAS detector." *Journal of Physics conference series* **10** 645:012023
- [5] Liao S, Erasmus R, Jivan H, Pelwan C, Peters G, Sideras-Haddad E. 2015. "A comparative study of the radiation hardness of plastic scintillators for the upgrade of the Tile Calorimeter of the ATLAS detector." *Journal of Physics conference series* **10** 645:012021
- [6] Bisanti P 1986 "Magnetic properties of matter" *Turin:World Scientific* ed Borsa F, Tognetti V p 385-408
- [7] Chen M 2011 "Radiation detectors II: Scintillation detectors." [Online] Available: [www.physics.queensu.ca/phys352/](http://www.physics.queensu.ca/phys352/)
- [8] Bulavin M. 2015 Irradiation facility at the IBR-2 reactor for investigation of material radiation hardness *Nuclear Instruments and Methods* **B343** p26 - 29.
- [9] Los Alamos National Laboratory [Online] Available:<http://mcnp.lanl.gov/mcnp5.shtml> [Accessed 24 06 2017]